



# Atomistic-continuum modeling of dislocation interaction with $Y_2O_3$ particles in iron

Akiyuki Takahashi<sup>a,\*</sup>, Zhengzheng Chen<sup>b</sup>, Nasr Ghoniem<sup>c</sup>, Nicholas Kioussis<sup>b</sup>

<sup>a</sup> Tokyo University of Science, 2641 Yamazaki, Noda-shi, Chiba 278-8510, Japan

<sup>b</sup> California State University at Northridge, 18111 Nordhoff Street, Northridge, CA 91330, United States

<sup>c</sup> California University at Los Angeles, Los Angeles, CA 90095, United States

## ARTICLE INFO

### Article history:

Available online 24 December 2010

## ABSTRACT

Oxide dispersion strengthened (ODS) steels are promising candidates for applications in fusion and fission reactors.  $Y_2O_3$  particles dispersed in an iron matrix drastically improve the strength without adverse effects on ductility. We investigate here details of the dislocation core structure in  $Y_2O_3$  precipitates, and at the interface between the iron matrix and the  $Y_2O_3$  precipitate. We also simulate dislocation interaction with nano-size  $Y_2O_3$  precipitates. It is shown that the  $\gamma$ -surface energies on planes between oxygen atoms and metallic atoms are extremely high, and that dislocations in an iron matrix cannot penetrate into  $Y_2O_3$  particles. Three-dimensional parametric dislocation dynamics simulations of the interaction between an edge dislocation and an  $Y_2O_3$  particle are carried out. The results show that the critical resolved shear stress (CRSS) has a strong dependence on the lattice mismatch  $Y_2O_3$  particles and the iron matrix, and that it is lower than analytically calculated values of the Orowan stress.

© 2010 Elsevier B.V. All rights reserved.

## 1. Introduction

Oxide dispersion strengthened (ODS) steels are promising candidates as structural materials for applications in fusion and fission reactors. In ODS steels,  $Y_2O_3$  particles dispersed in an iron matrix drastically improve the strength, without adverse effects on ductility.  $Y_2O_3$  particles work as obstacles to dislocation motion, resulting in an increase in the flow stress for plastic deformation. Despite the important effects of  $Y_2O_3$  precipitates on the mechanical properties of ODS steels, a mechanistic understanding of the interaction between dislocations and such precipitates is not available yet.

In this work, we first model the dislocation core structure in  $Y_2O_3$  particles and at the interface between the iron matrix and these precipitates on the basis of the information on  $\gamma$ -surface energies. We then simulate the dislocation penetration from the iron matrix to the  $Y_2O_3$  particle through the interface using a combination of 2-dimensional dislocation dynamics (DD) and generalized Peierls-Nabarro (GPN) model [1]. This hybrid method is capable of resolving the dislocation core structure, and was presented by our groups in a number of publications [1–3]. We will show, on the basis of the hybrid method, that the possibility of dislocation penetration through  $Y_2O_3$  particles is negligible. We develop a 3-dimensional parametric dislocation dynamics (PDD) simulation model [4] for investigation of the interaction between an edge dislocation and  $Y_2O_3$  particles. Using PDD simulations,

dislocation behavior in the vicinity of  $Y_2O_3$  particles and the critical resolved shear stress (CRSS) for dislocations to overcome  $Y_2O_3$  precipitates are investigated.

## 2. $\gamma$ -Surface energies in $Y_2O_3$ particles and interfaces

To investigate the interaction between dislocations in iron with  $Y_2O_3$  precipitates, we first investigated possible types of interfaces between an iron matrix and  $Y_2O_3$  particles, and found that  $\{1\ 0\ 0\}$  planes of both the iron matrix and  $Y_2O_3$  particles provide the best matching. Therefore, the interaction between dislocations and the  $\{1\ 0\ 0\}$  interface will be determined in order to discuss dislocation behavior in the vicinity of the interface. One possible slip system in  $Y_2O_3$  precipitates is  $\{1\ 0\ 0\}\langle 1\ 1\ 0\rangle$ , which differs from those in the iron matrix, namely  $\{1\ 1\ 0\}\langle 1\ 1\ 1\rangle$ . Therefore, if a dislocation meets the interface, it would have to change its slip system in order to penetrate the  $Y_2O_3$  particle. To understand the dislocation core structure at the interface,  $\gamma$ -surface energies, which represent interplanar atomic misfit energies and are responsible for determining the dislocation core structure in the  $Y_2O_3$  particle and the interfaces were calculated using *ab initio* methods with the Vienna *Ab initio* Simulation Package (VASP) code [5,6]. Here, we assumed two different interfaces. The first is the iron–oxygen interface, where the oxygen atoms are placed at the bonding surface of  $Y_2O_3$ . Similarly, the second is the iron–yttrium interface, where there are yttrium atoms at the bonding surface of  $Y_2O_3$ . The results are shown in Fig. 1, where the maximum  $\gamma$ -surface energy at the iron–yttrium interface is less than  $1\text{ J/m}^2$ . However, when the slip plane contains oxygen atoms, the  $\gamma$ -surface energy rises up significantly to approximately  $4\text{ J/m}^2$  at the iron–oxygen interface and,

\* Corresponding author. Tel.: +81 4 7122 1165; fax: +81 4 7123 9814.

E-mail addresses: [takahash@rs.noda.tus.ac.jp](mailto:takahash@rs.noda.tus.ac.jp) (A. Takahashi), [ghoniem@ucla.edu](mailto:ghoniem@ucla.edu) (N. Ghoniem), [nick.kioussis@csun.edu](mailto:nick.kioussis@csun.edu) (N. Kioussis).

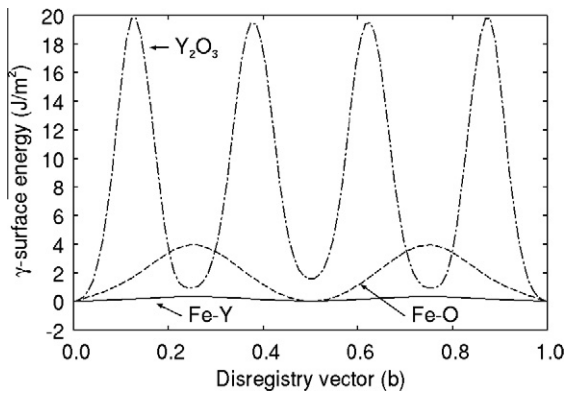


**Fig. 1.**  $\gamma$ -Surface energies of interfaces between iron and oxygen and between iron and yttrium and  $\text{Y}_2\text{O}_3$ . The disregistry vector is the displacement vector making the atomic misfit plane. In this figure, the vector is taken as the Burgers vector, and the plane is the slip plane of dislocations.

in  $\text{Y}_2\text{O}_3$ , the  $\gamma$ -surface energy increases drastically to  $20 \text{ J/m}^2$ . The main reason for such high energy barriers to slip is that the dislocation must break ionic bonds between oxygen and metal atoms, which results in very strong resistance to dislocation motion.

### 3. Dislocation-interface interactions

When dislocations meet the interface, they must change their slip system in order to penetrate the  $\text{Y}_2\text{O}_3$  particle. The  $\{110\}$   $\langle 111 \rangle$  dislocation in the iron matrix may dissociate into a  $\{100\}$   $\langle 100 \rangle$  dislocation on the interface and a  $\{100\}$   $\langle 110 \rangle$  dislocation in the  $\text{Y}_2\text{O}_3$  particle. The lattice constants of iron and  $\text{Y}_2\text{O}_3$  are  $a_0^{\text{Fe}} = 0.28865 \text{ nm}$  and  $a_0^{\text{Y}_2\text{O}_3} = 1.0605 \text{ nm}$ , respectively [7]. To simplify the dislocation reaction at the interface, we take the lattice constants of iron and  $\text{Y}_2\text{O}_3$  to be  $a_0^{\text{Fe}} = 0.275 \text{ nm}$  and  $a_0^{\text{Y}_2\text{O}_3} = 1.100 \text{ nm}$ . Using these approximate lattice constants, 8 dislocations in the iron matrix can create one dislocation in the  $\text{Y}_2\text{O}_3$  particle.

The interaction between the dislocation and the  $\text{Y}_2\text{O}_3$  particle is simulated using a hybrid of 2-dimensional DD and the GPN model. The method can simulate not only the dislocation structure at rest, but it can also determine the dislocation core structure during the interaction with precipitates or other defects. Details of the hybrid DD-GPN model can be found elsewhere [1]. Fig. 2a shows a sketch of the simulation model used for the present investigations. Since the simulation model is similar to the structure of bi-material, it is difficult to account for the influence of elastic constant mismatch in the hybrid DD-GPN model. However, the difference in the elastic constants between the two materials is not substantial [6] so that we ignore here the influence. The  $x$  and  $y$  axes are along the  $[110]$ - and  $[1\bar{1}0]$ -directions, respectively. Initially, 8 mixed dislocations are discretized with 80 fractional dislocations for the GPN model, and are then introduced into the iron matrix. The interface lies along the  $(010)$  plane, and its trace has an angle of  $45^\circ$  with the  $x$ -axis. In the simulation, two different types of interfaces are considered: (1) iron and oxygen and (2) iron–yttrium. The dislocations in the iron matrix have a  $a_0^{\text{Fe}}/2[111]$  Burgers vector, and dissociate into two different dislocations on the interface and inside the  $\text{Y}_2\text{O}_3$  particle. The applied stress tensor is  $\sigma_x = \sigma_y = \sigma_{yz} = \sigma_{xz} = \bar{\sigma}$ ,  $\sigma_z = \sigma_{xy} = 0$ , where  $\bar{\sigma}$  is a prescribed stress value. The selected stress state facilitates dislocation glide in the iron matrix, at the interface and inside the  $\text{Y}_2\text{O}_3$  particle.

Fig. 2 shows snapshots of fractional dislocation distributions (which represent the distributed dislocation core in the GPN model [1–3]), for an applied shear stress of  $\bar{\sigma} = 150 \text{ GPa}$ . In the simulation (Fig. 2), the interface is composed of iron and oxygen atoms, and

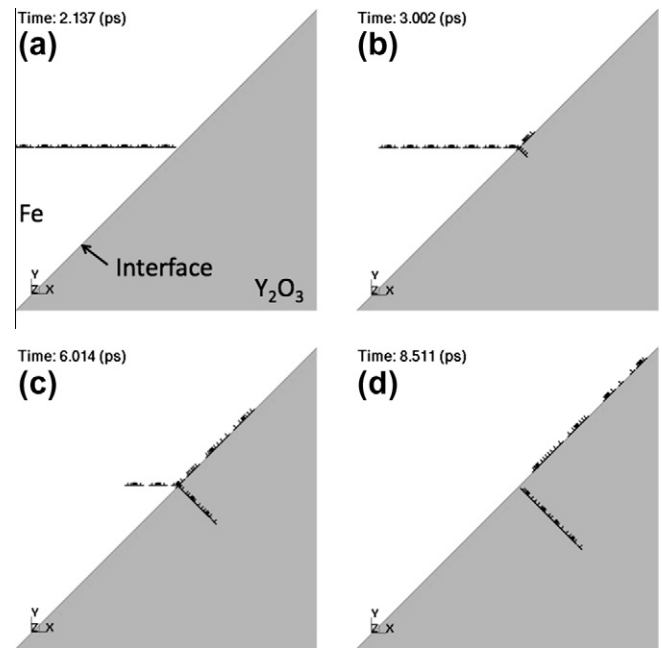


**Fig. 2.** Snapshots of the dislocation–interface interaction process. The applied shear stress is  $150 \text{ GPa}$ . The interface is composed of iron–oxygen. The slip system of the interface is  $(010)[100]$ , and in the  $\text{Y}_2\text{O}_3$  is  $(100)[011]$ .

the dislocations in the iron matrix dissociate into two dislocations with Burgers vectors of  $a_0^{\text{Y}_2\text{O}_3}/2[100]$  (on the interface) and  $a_0^{\text{Y}_2\text{O}_3}/2[011]$  (in the  $\text{Y}_2\text{O}_3$  particle). It is shown in the figure that the dislocation core in the iron matrix moves toward the interface and successfully dissociates into two different dislocations in the interface and in the  $\text{Y}_2\text{O}_3$  particle. Finally, the dislocation core in the iron matrix penetrates the  $\text{Y}_2\text{O}_3$  particle. As a result, the critical stress necessary for dislocations to completely pass the iron–yttrium interface is found to be  $21 \text{ GPa}$ , while, for the iron–oxygen interface, it is  $128 \text{ GPa}$ , which is large compared to the case of iron–yttrium interface. The trend coincides with the magnitude of the  $\gamma$ -surface energies. However, most importantly, the required stress is unrealistically large in all cases, exceeding the shear modulus of both Fe and  $\text{Y}_2\text{O}_3$ . This leads us to conclude that dislocations in the iron matrix cannot penetrate  $\text{Y}_2\text{O}_3$  particles under realistic shear stresses, and thus must form Orowan loops around the precipitates.

### 4. Critical resolved shear stress for dislocation- $\text{Y}_2\text{O}_3$ particle interactions

In this section, we determine the CRSS for dislocations to pass  $\text{Y}_2\text{O}_3$  particles by the Orowan mechanism, using self-consistent 3-dimensional PDD and boundary element methods (BEM), as developed by Takahashi and Ghoniem for the elastic interaction between dislocations and precipitates [3]. In the present simulations with the self-consistent PDD-BEM technique [3], the dislocation is allowed to stop at the interface, which will naturally provide the well-known Orowan mechanism. Moreover, the elastic interaction between the dislocations and the  $\text{Y}_2\text{O}_3$  particle arising from differences in the elastic constants and the lattice mismatch are all accounted for. As explained in the previous section, although the influence of the elastic constants must be negligibly small, we account for the influence to get more precise solution of the interaction. The lattice mismatch strain is calculated from the lattice constants of iron and  $\text{Y}_2\text{O}_3$ , and is found to be  $-0.0752$  [7].

Fig. 3 shows a sketch of the simulation model, where the  $x$ ,  $y$  and  $z$  axis are along the  $[11\bar{2}]$ ,  $[111]$  and  $[1\bar{1}0]$  orientations,

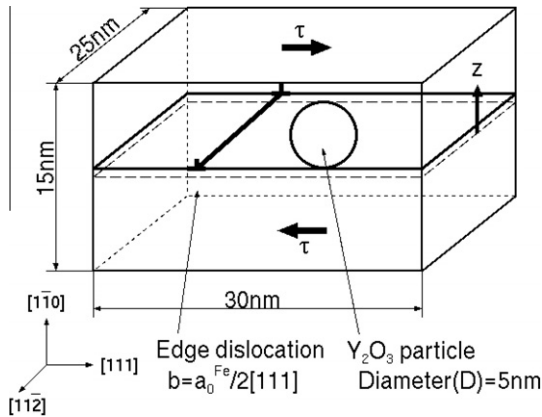


Fig. 3. Simulation model for the interaction between an edge dislocation and an  $Y_2O_3$  particle in iron.

respectively. The size of the simulation volume is  $25 \times 15 \times 30$  nm. In the simulation model, a spherical  $Y_2O_3$  particle with a diameter  $D = 5$  nm is located at the center of the simulation volume. Because the diameter of the particle is small, the particle is assumed to be coherent with the iron matrix. The particle is represented with boundary and volume elements in the simulations. An edge dislocation is also located in the simulation volume. The slip plane of the dislocation is the  $(1\bar{1}0)$  plane, and the position is advanced along  $[1\bar{1}0]$  to determine the dependence of the CRSS on the dislocation position.

Fig. 4 shows snapshots of the dislocation configuration during its interaction with the nano-size precipitate, for a slip plane position of  $z/D = -0.6$ . The  $Y_2O_3$  particle has a negative coherency strain, which provide tension stress in the  $Y_2O_3$  particle. At the beginning of the interaction, the dislocation is attracted to the precipitate, because most of the  $Y_2O_3$  particle volume is on the compression side of dislocation. Then the dislocation contacts the front of the  $Y_2O_3$  particle, and starts to form an Orowan loop. How-

ever, the dislocation cannot complete forming the Orowan loop, because the character of the elongated part of dislocation surrounding the  $Y_2O_3$  particle differs from that of the initial edge dislocation, which changes the type of interaction from attractive to repulsive. This repulsive interaction is a strong impediment to the formation of the Orowan loop.

Fig. 5 shows snapshots of the dislocation configuration, where the slip plane position is  $z/D = 0.6$ . In this case, most of the  $Y_2O_3$  particle volume is on the tension side of the dislocation so that the dislocation and the  $Y_2O_3$  particle initially have a repulsive interaction. As a result, the dislocation cannot contact the front of the  $Y_2O_3$  particle. As the dislocation moves further, it can form a full Orowan loop around the  $Y_2O_3$  particle, as shown in the figure. In contrast to the  $z/D = -0.6$  case, the character of the elongated part of dislocation changes from that of the initial edge dislocation, and the interaction changes from repulsive to attractive. Such attractive interaction of the elongated dipole around the precipitate should accelerate the formation of the Orowan loop. This can be clearly seen in the shape of the Orowan loop around the  $Y_2O_3$  particle (Fig. 5d).

Fig. 6 shows the dependence of the CRSS on the vertical distance off the precipitate mid-plane. Also, the Orowan stress calculated as  $\mu b/L_0$  is plotted in the figure, where  $\mu$  is the elastic shear modulus of iron,  $b$  is the Burgers vector and  $L_0$  is the spacing between the  $Y_2O_3$  particles on the slip plane of dislocation. In the figure, the CRSS at all slip planes is lower than that calculated analytically by 10–100%, depending on the slip plane location. The Orowan stress is inversely proportional to  $L_0$  so that the maximum Orowan stress appears when the position of the slip plane is  $z/D = 0$ . However, the simulation results indicate that the maximum CRSS appears at  $z/D = -0.2$ , which differs from the analytically estimated position for the maximum CRSS. As can be seen in the snapshots of the simulations (Figs. 4 and 5), the dislocation has a strong elastic interaction with the  $Y_2O_3$  particle, mainly caused by the lattice mismatch. The results shown in Fig. 6 indicate that the CRSS is an asymmetric function of the dislocation position relative to the slip plane, which is explained as follows. When the position of slip plane  $z/D$  is negative, the dislocation has an attractive interaction

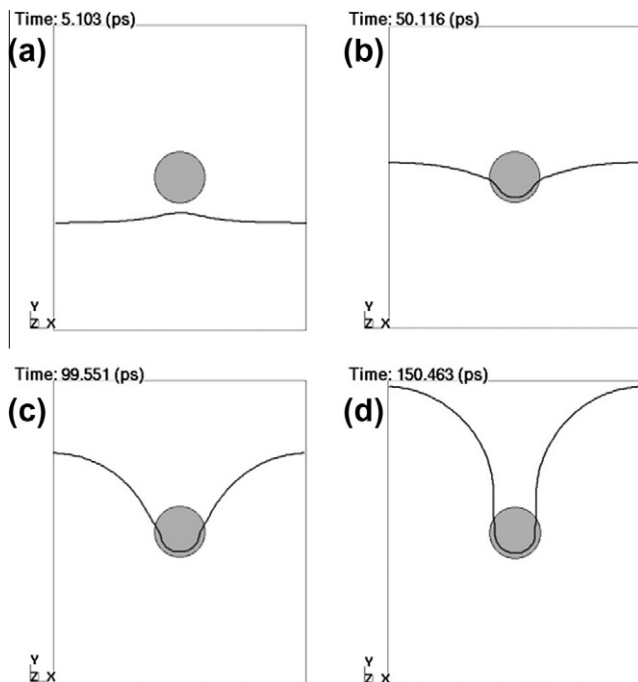


Fig. 4. Snapshots of the dislocation- $Y_2O_3$  particle interaction process. The position of slip plane is  $z/D = -0.6$ .

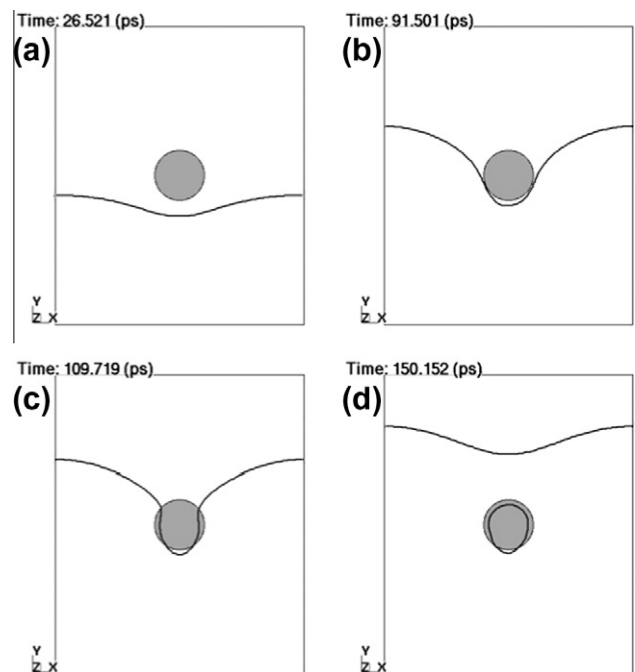


Fig. 5. Snapshots of the dislocation- $Y_2O_3$  particle interaction process. The position of slip plane is  $z/D = 0.6$ .

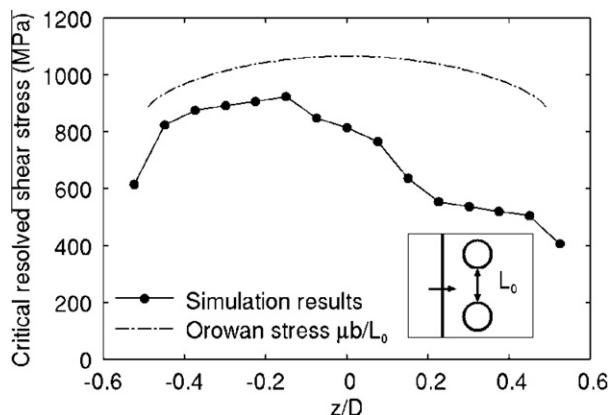


Fig. 6. Critical resolved shear stress for dislocations to clear  $Y_2O_3$  particles. The dashed line is an analytically calculated Orowan stress.

with the  $Y_2O_3$  particle. However, at later stages of the Orowan mechanism, the interaction changes to a repulsive one, rendering it difficult to complete the Orowan mechanism. Therefore, the repulsive interaction increases the CRSS compared to the original Orowan stress. On the other hand, as the position of slip plane  $z/D$  becomes positive, the CRSS decreases rapidly. This must also be the influence of the lattice mismatch on the interaction. When the slip position is positive, the interaction is initially repulsive, and then changes to attractive at a later stage of the Orowan mechanism. The attractive interaction should assist the formation of Orowan loops around  $Y_2O_3$  particles. Thus the CRSS becomes smaller as a consequence of the influence of the lattice mismatch.

## 5. Conclusions

We first performed *ab initio* calculations of  $\gamma$ -surface energies in an iron matrix, for the interface between Fe and  $Y_2O_3$  precipitates and for slip planes inside  $Y_2O_3$  particles. Based on the results of *ab initio* calculations, 2-dimensional DD simulations of dislocation core structure and penetration through interfaces and precipitates were carried out. Finally, 3-dimensional PDD simulations of the interaction between a dislocation and a spherical  $Y_2O_3$  particle were performed to investigate dislocation interaction and configu-

ration in the vicinity of  $Y_2O_3$  particles, and to determine and the CRSS. Through these studies, we conclude the following:

- (1) The  $\gamma$ -surface energies of the iron–oxygen interface and on slip planes in  $Y_2O_3$  precipitates are extremely large, resulting in pronounced resistance to slip at the interface and inside the nano-size precipitates. This is a consequence of the ionic bond between oxygen and metallic atoms.
- (2) The stress necessary for dislocations to penetrate the interface is unrealistically large. This is attributed to the large  $\gamma$ -surface energies of the iron–oxygen interface and in the  $Y_2O_3$ . Therefore, dislocations will stop their motion at the interface of the  $Y_2O_3$  particle, and perform Orowan looping to go over  $Y_2O_3$  particles.
- (3) The CRSS for the interaction is a function of the slip plane position with respect to the precipitate mid-plane, as a consequence of the lattice mismatch between the iron matrix and the  $Y_2O_3$  particle. Orowan looping becomes easier when most of the  $Y_2O_3$  particle volume is located on the tension side of the dislocation, because the lattice mismatch strain assists the formation of the Orowan loop around the  $Y_2O_3$  particle. Unlike analytical estimates for the Orowan stress, the present results show an asymmetry in the CRSS as a function of the vertical position of the slip plane from the precipitate mid-plane.

## Acknowledgements

The authors acknowledge the support of the US Department of Energy, Office of Fusion Energy for research at UCLA through Grant # DE-FG02-03ER54708, and the US Department of Energy, Office of Nuclear Energy for research support at UCLA and at CSUN through the NERI Grant # DE-FC07-06ID14748.

## References

- [1] S. Banerjee, N.M. Ghoniem, G. Lu, N. Kioussis, *Philos. Mag.* 87 (2007) 4131–4150.
- [2] M.A. Shehadeh, G. Lu, S. Banerjee, N. Kioussis, N. Ghoniem, *Philos. Mag.* 87 (10) (2007) 1513–1529.
- [3] A. Takahashi, N.M. Ghoniem, *J. Mech. Phys. Solids* 56 (2008) 1534–1553.
- [4] N.M. Ghoniem, S.-H. Tong, L.Z. Sun, *Phys. Rev. B* 61 (2000) 913–927.
- [5] G. Kresse, J. Hafner, *Phys. Rev. B* 47 (1993) 558–561.
- [6] G. Kresse, J. Hafner, *J. Phys.: Condens. Mater.* 6 (1994) 8245–8257.
- [7] R.J. Gaboriaud, M. Boisson, *J. de Phys.* 41 (C6) (1980) 171–174.